Articles

Nitrogenase of *Azotobacter vinelandii*: Kinetic Analysis of the Fe Protein Redox Cycle†

Martina G. Duyvis, Hans Wassink, and Huub Haaker*

Laboratory of Biochemistry, Department of Biomolecular Sciences, Wageningen Agricultural University, Dreijenlaan 3, 6703 HA Wageningen, The Netherlands

Received June 25, 1998; Revised Manuscript Received October 12, 1998

ABSTRACT: Nitrogenase consists of two metalloproteins (Fe protein and MoFe protein) which are assumed to associate and dissociate to transfer a single electron to the substrates. This cycle, called the Fe protein cycle, is driven by MgATP hydrolysis and is repeated until the substrates are completely reduced. The rate-limiting step of the cycle, and substrate reduction, is suggested to be the dissociation of the Fe protein−MoFe protein complex which is obligatory for the reduction of the Fe protein [Thorneley, R. N. F., and Lowe, D. J. (1983) *Biochem. J. 215*, 393−403]. This hypothesis is based on experiments with dithionite as the reductant. We also tested besides dithionite flavodoxin hydroquinone, a physiological reductant. Two models could describe the experimental data of the reduction by dithionite. The first model, with no reduction of Fe protein bound to MoFe protein, predicts a rate of dissociation of the protein complex of 8.1 s^{-1}. This rate is too high to be the rate-limiting step of the Fe protein cycle ($k_{obs} = 3.0$ s^{-1}). The second model, with reduction of the Fe protein in the nitrogenase complex, predicts a rate of dissociation of the protein complex of 2.3 s^{-1}, which in combination with reduction of the nitrogenase complex can account for the observed turnover rate of the Fe protein cycle. When flavodoxin hydroquinone (155 μM) was the reductant, the rate of reduction of oxidized Fe protein in the nitrogenase complex ($k_{obs} \approx 400$ s^{-1}) was 100 times faster than the turnover rate of the cycle with flavodoxin as the reductant (4 s^{-1}). Pre-steady-state electron uptake experiments from flavodoxin hydroquinone indicate that before and after reduction of the nitrogenase complex relative slow reactions take place, which limits the rate of the Fe protein cycle. These results are discussed in the context of the kinetic models of the Fe protein cycle of nitrogenase.

The biological reduction of dinitrogen to ammonia is catalyzed by nitrogenase, which consists of two metalloproteins that are both necessary for catalysis (*1*). For the complete reduction of N_2 to $2NH_3$ and H_2 (a side product of the nitrogenase reaction), a strong reductant (flavodoxin or ferredoxin in vivo and sodium dithionite in vitro) and MgATP, which is hydrolyzed during catalysis, must be present. In this investigation, the molybdenum-containing nitrogenase from *Azotobacter vinelandii* is studied. The MoFe protein,[1] a heterodimer of 230 kDa, contains two types of metal−sulfur clusters per $\alpha\beta$-monomer: the FeMo cofactor (FeMoco) and the P-cluster. FeMoco is generally considered to be the substrate reduction site. The P-cluster might be involved in electron transfer from the Fe protein to FeMoco (*2*−*4*). Structural models for FeMoco and the P-cluster have been proposed, on the basis of crystallographic analysis of the MoFe protein (*5*−*7*). The Fe protein is a homodimer of 63 kDa, which contains a single [4Fe-4S] cluster and two nucleotide-binding sites. The crystallographic structure of the *A. vinelandii* Fe protein was determined by Georgiadis et al. (*8*). The crystal structure and site-directed mutagenesis studies of the Fe protein revealed that the nucleotide binding region of the Fe protein is highly similar to the nucleotide binding region of the H-*ras* p21 protein (*8*, *9*). The H-*ras* p21 protein is a member of the group of nucleotide-switch proteins, like myosin (*10*), and the heterotrimeric G proteins (*11*, *12*). These proteins use the binding and hydrolysis of nucleotides to switch

† This investigation was supported by The Netherlands Foundation for Chemical Research (SON) with financial aid from The Netherlands Organization for Scientific Research (NWO).

* To whom correspondence should be addressed. Telephone: +31 317486828. Fax: +31317484801. E-mail: Huub.Haaker@nitro.bc.wau.nl.

[1] Abbreviations: MoFe protein, molybdenum−iron protein of nitrogenase; Fe protein, iron protein of nitrogenase; FeMoco, iron−molybdenum−sulfur−homocitrate cofactor of nitrogenase; P-cluster, [8Fe-7S] cluster of nitrogenase; P^N and P^{2+}, dithionite-reduced and two-electron-oxidized P-cluster, respectively; Av1 and Av2, MoFe protein and Fe protein of *A. vinelandii* nitrogenase, respectively; Kp1 and Kp2, MoFe protein and Fe protein of *K. pneumoniae* nitrogenase, respectively; Ac2, Fe protein of *Azotobacter chroococcum* nitrogenase; $Av2_{ox}$ and $Av2_{red}$, oxidized and reduced Av2, respectively; $Av2(MgADP)_2$, Av2 with two MgADP bound; Fld_{HQ} and Fld_{SQ}, flavodoxin hydroquinone and semiquinone, respectively.

10.1021/bi981509y CCC: $15.00
Published on Web 11/20/1998

Scheme 1: Fe Protein Cycle (Adapted from Ref *26*)[a]

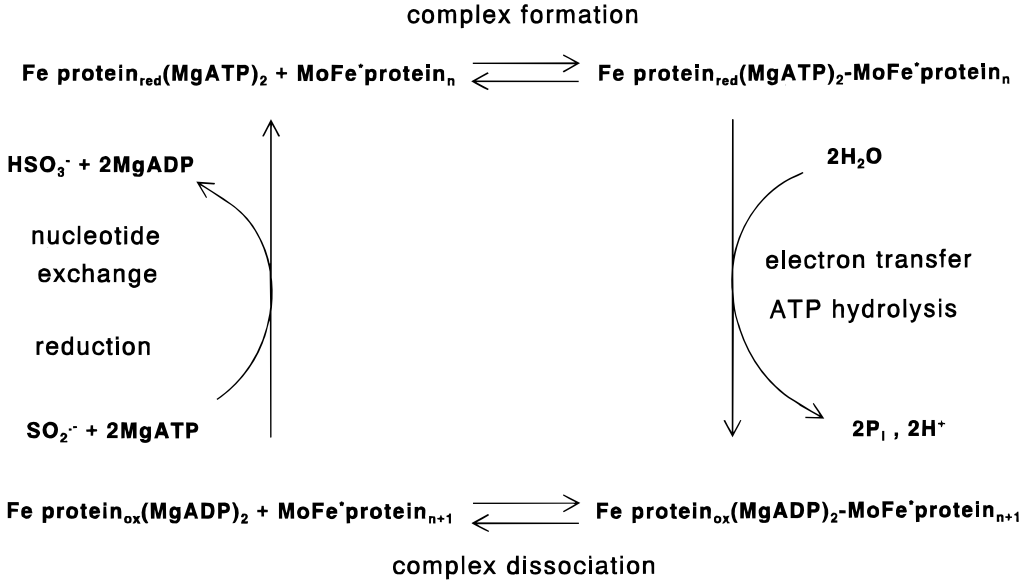

[a] The MoFe*protein is one of the two independently functioning halves of the MoFe protein. The MoFe* protein$_n$ is the MoFe protein reduced by *n* electrons.

between two different protein conformations, which determines whether the protein triggers a biochemical process. The transition state of the nucleoside triphosphate hydrolysis reaction of myosin and of the heterotrimeric G proteins could be stabilized by the combination of the nucleoside diphosphate and aluminum fluoride. The two-component protein complex of nitrogenase (*13*, *14*) and the two-component nucleotide-switch protein H-*ras* p21 and its GTPase-activating protein (GAP) bind only aluminum fluoride when the nucleoside diphosphate and both component proteins are present (*15*). Later, it was shown that the structures of the ADP·AlF_4^--stabilized nitrogenase complex (*16*) and the Ras·GDP·AlF_4^-·GAP complex (*17*) also resemble that of the transition state of the nucleotide hydrolysis reaction of the nucleotide-switch proteins (*10*−*12*).

Similar to the case for the nucleotide-switch proteins, conformational changes of the nitrogenase protein complex have been proposed as the basis of the ATP hydrolysis-driven unidirectional electron transfer from the Fe protein to FeMoco at the MoFe protein (*1*, *9*). Up to now, three stable homologous Fe protein−MoFe protein complexes have been identified and (partly) characterized. The structure of the ADP·AlF_4^--stabilized nitrogenase complex resembles an intermediate of the on-enzyme MgATP hydrolysis reaction (*16*). By using altered Fe proteins, nondissociating nitrogenase complexes could be prepared. The deletion of Leu at position 127 of the Fe protein (L127Δ) generates an Fe protein that resembles the Fe protein in the MgATP-bound state (*18*). The L127Δ Fe protein binds very tightly to the MoFe protein and slowly transfers one electron to the MoFe protein without MgATP (*19*). The midpoint potentials of the L127Δ Fe protein [4Fe-4S]$^{2+/+}$ cluster and of the two-electron-oxidized couple of the P-cluster ($P^{2+/N}$) of the MoFe protein in the protein−protein complex are lowered. This indicates that the complex represents a conformation which induces electron transfer to FeMoco (*20*). Another stable protein−protein complex could be made between the D39N Fe protein and the MoFe protein. In the D39N Fe protein, aspartate 39 was changed into an asparagine. This amino acid is part of the putative protein chain that connects the nucleotide-binding site to the MoFe protein-docking surface of the Fe protein. In the nitrogenase complex formed between the D39N Fe protein and the MoFe protein, a MgATP-dependent electron transfer takes place, which is not followed by further redox reactions. Since this protein−protein complex does not dissociate, it is suggested that electron transfer within the nitrogenase complex normally induces conformational changes, which increase the affinity of the Fe protein for the MoFe protein. The D39N Fe protein lacks the ability to change the nitrogenase complex from this conformation to the MgADP-bound conformation which is necessary for dissociation of the nitrogenase complex (*21*). Besides this recently obtained structural information about the different protein−protein complexes, kinetic studies have also provided insight into the different reactions of the MgATP hydrolysis-driven electron transfer reactions. Hageman and Burris (*22*) first proposed that the redox cycle of nitrogenase is a single electron transfer event and that the nitrogenase complex must dissociate after the transfer of each electron from the Fe protein to the MoFe protein, implying that for substrate reduction several cycles of association and dissociation of the nitrogenase proteins are necessary. Thorneley and Lowe (*23*−*25*) further developed the kinetic description of nitrogenase. They proposed a model (based on kinetic data for *Klebsiella pneumoniae* nitrogenase, with sodium dithionite as the reductant) which comprises two cycles of electron transfer called the Fe protein cycle and the MoFe protein cycle. In the Fe protein cycle (Scheme 1), after formation of the nitrogenase complex, one electron is transferred from the reduced Fe protein to the MoFe protein with concomitant hydrolysis of MgATP. Subsequently, the nitrogenase complex dissociates into the separate nitrogenase proteins, which is the rate-limiting step of the nitrogenase reaction when all reactants are at saturating levels (*23*). After dissociation of the complex, the electron donor reduces the Fe protein and MgADP is rapidly replaced by MgATP (26). The MoFe protein cycle describes the stepwise reduction of the MoFe protein by succeeding Fe protein

cycles, up to a maximal reduction level of eight electrons, necessary to complete the reduction of dinitrogen to ammonia and hydrogen (*24*, *25*, *27*).

In the original scheme of the Fe protein cycle, electron transfer and MgATP hydrolysis are represented by one reaction, but it is obvious that during the course of MgATP hydrolysis several events will take place that trigger or cause conformational changes in the protein−protein complex. Kinetic data have become available for different events in this part of the Fe protein cycle; the MgATP conformation of the nitrogenase complex allows electron transfer from the Fe protein to the MoFe protein (*19*, *28*), and the on-enzyme hydrolysis of MgATP, detected as a delay reaction, is followed by a conformational change (*29*) and H^+ and P_i release (*28*, *30*). Another conformational change might be necessary for dissociation of the nitrogenase complex (*21*). The aim of this work is to describe kinetically the last part of the Fe protein cycle, the re-reduction of the Fe protein. To that end, several reactions of the Fe protein cycle were studied. These reactions include the proposed rate-limiting step of the Fe protein cycle, dissociation of the nitrogenase complex, and the reduction of the oxidized Fe protein with MgADP bound. Two reductants were tested: sodium dithionite and flavodoxin hydroquinone. With flavodoxin, it is possible to monitor spectroscopically the pre-steady-state and steady-state uptake of electrons by nitrogenase. Evidence will be presented that flavodoxin hydroquinone is able to reduce the nitrogenase protein complex after the MgATP-induced electron transfer and before dissociation of the nitrogenase complex. These results will be discussed in the context of models of the Fe protein cycle of nitrogenase.

MATERIALS AND METHODS

Cell Growth, Isolation, and Preparation of Nitrogenase. *A. vinelandii* ATCC strain 478 was grown, and the separate nitrogenase proteins were isolated as described by Mensink et al. (*31*). The molar concentrations of the *A. vinelandii* MoFe protein (Av1) and Fe protein (Av2) were determined from their molecular masses of 230 and 63 kDa, respectively. The activities of the nitrogenase components were determined from their specific acetylene reduction activity (*32*). The specific activities of the Av1 and Av2 preparations used in the experiments were at least 8 mol of ethylene produced s^{-1} (mol of protein)$^{-1}$ and 2 mol of ethylene produced s^{-1} (mol of protein)$^{-1}$, respectively. Av1 contained 1.8 ± 0.2 mol of Mo/mol of Av1; the Fe content of Av2 was 3.7 ± 0.2 mol of Fe/mol of Av2.

Dithionite-free Av1 was prepared by running the protein over a Biogel P-6DG column (Bio-Rad, 1 cm × 8 cm), which was equilibrated with argon-saturated 10 mM $MgCl_2$ and 100 mM NaCl in 50 mM Tes/NaOH (pH 7.4). Dye-oxidized Av2 was prepared with phenazine methosulfate (PMS), following a published procedure (*31*). Flavodoxin II from *A. vinelandii* was isolated as described earlier (*33*).

Chemicals. ADP and ATP (special quality) were obtained from Boehringer; PMS was obtained from Sigma, and sodium dithionite was from Merck and contained 20% sodium sulfite. The concentration of $SO_2^{\bullet-}$ was calculated from the concentration of dithionite using the dissociation constant of the reaction $S_2O_4^{2-} \leftrightarrow 2SO_2^{\bullet-}$ of 1.4×10^{-9} M (*34*).

Stopped-Flow Experiments. The stopped-flow experiments were performed with a Hi-TECH SF-51 stopped-flow spectrophotometer, equipped with an anaerobic kit and a data acquisition and analysis system. All experiments were performed at 20.0 ± 0.1 °C, under argon. The mixing ratio was 1:1. In the calculation of the absorbance changes, a dead reaction time of 1.5 ms was taken into account, which was determined from the rate of the reduction of dichlorophenolindophenol by ascorbate, under appropriate conditions.

The electron transfer from Av2 to Av1 in the presence of flavodoxin was assessed by monitoring the absorbance changes at 418 nm instead of at 430 nm. The wavelength of 418 nm was chosen, since flavodoxin (Fld_{HQ}/Fld_{SQ}) has an isosbestic point at this wavelength. The extent of electron uptake by nitrogenase during turnover was measured by monitoring the oxidation of flavodoxin hydroquinone to semiquinone at 580 nm using a value for the molecular absorbance coefficient ϵ_{580} of 5.7 mM^{-1} cm^{-1} (*33*).

Determination of the Rate of Reduction of Oxidized Av2. The standard buffer used in the stopped-flow experiments, designed to determine the rate of reduction of $Av2_{ox}$, contained 1 mM ADP, 10 mM $MgCl_2$, 50 mM NaCl, and 50 mM Tes/NaOH (final pH of 7.4). The ionic strength of this solution was equal to that of 109 mM NaCl. When sodium dithionite was present at concentrations above 5 mM, the concentration of NaCl in the dithionite-containing syringe of the stopped-flow apparatus was lowered to keep the ionic strength constant.

The rate of dissociation of the nitrogenase complex, Av1·$Av2_{ox}(MgADP)_2$, was determined as described for nitrogenase from *K. pneumoniae* (*23*). The simulations were performed with KINSIM (*35*) and FITSIM (*36*). The programs were obtained from the KINSIM site at 128.252.135.4. The simulated data points were fit to the experimental data by nonlinear regression. The quality of the fit between the simulated data and the experimental data curves is reflected in the R^2 value (a value of 1 indicates a perfect fit) and the mean square error (MSE), which is the sum of the squared differences between the experimental and calculated data points, divided by the amount of variables used in the simulation, and should be close to 0.

Determination of the Rate of Turnover. The rate of nitrogenase turnover at 20 °C was obtained from the rate of H_2 formation. The reaction mixture contained 0.55 μM Av1, 11.0 μM Av2, and an ATP-regenerating system as described by Braaksma et al. (*32*). We used 20 mM sodium dithionite or 50 μM flavodoxin and 5 mM sodium dithionite as the reductant. Higher flavodoxin concentrations did not stimulate the nitrogenase activity. From the rate of H_2 production, the turnover rate of the Fe protein cycle was calculated assuming the transfer of one electron per cycle. The ionic strength of the assay mixture was equal to that of a solution of 95 mM NaCl. Note that the ionic strength of the standard buffer used to determine kinetic constants of individual reactions of the Fe protein cycle is nearly the same as the ionic strength of the assay mixture used to determine the nitrogenase activity. This excludes possible effects of the ionic strength on the measured rates and rate constants.

RESULTS

Since the kinetic formulation of the Fe protein cycle (*22*−*24*), partial reactions of the ATP hydrolysis reaction have

been characterized. These are the pre-steady-state proton (*28*) and phosphate release (*30*) and a blue shift of the absorbance of the Fe−S clusters of oxidized nitrogenase (*29*). All three reactions show a lag of about 20 ms, and then a burst lasting 100 ms followed by an approach to a steady state. The observed kinetics are consistent with a rapid electron transfer reaction (100 s^{-1} for *Azotobacter* at 20 °C), a delay reaction (77 s^{-1}), and a blue shift of the absorbance of the Fe−S clusters and proton release reaction (14 s^{-1}) (*28*, *29*). The blue shift or proton and/or phosphate release reactions are not associated with the dissociation of the nitrogenase complex, which is supposed to be the rate-limiting step of the Fe protein cycle (*23*). The rate of dissociation can be determined by measuring the rate of the reduction of oxidized Fe protein with MgADP bound, in the presence of the MoFe protein. It is assumed that when the Fe protein is bound to the MoFe protein, the [4Fe-4S] cluster of the Fe protein cannot be reduced; therefore, the nitrogenase complex must dissociate first. To be able to perform a kinetic analysis of the data curves of the reduction of the nitrogenase complex, the kinetics of the reduction of the free Fe protein in the presence of MgADP must be determined.

Reduction of Oxidized Av2 with MgADP Bound by Sodium Dithionite. $Av2_{ox}$ was equilibrated with excess MgADP before mixing with dithionite and MgADP. It was verified that the level of binding of MgADP to $Av2_{ox}$ was saturating. The results from a typical experiment are shown in Figure 1A (trace 1). The rate of reduction of $Av2_{ox}(MgADP)_2$ by dithionite was monitored as a function of the concentration of dithionite (0.2−20 mM). The results are shown in Figure 1B. The amplitude of the single-exponential absorbance decrease was independent of the concentration of dithionite used. The millimolar absorption coefficient for the reduction of $Av2_{ox}(MgADP)_2$ at 430 nm was 3.53 ± 0.02 mM^{-1} cm^{-1}, while that of $Av2_{ox}$ was 4.50 ± 0.06 mM^{-1} cm^{-1}. Binding of MgADP lowers the redox potential of Av2 from −375 to −473 mV (*32*). A possible explanation for the lower extinction coefficient could be partial reduction. We therefore measured the potential of the redox buffer used with methyl viologen as an indicator as described by Deistung and Thorneley (*37*). The potential of a 5 mM $Na_2S_2O_4$ solution at pH 7.4 (4 mM $S_2O_4^{2-}$, 1 mM HSO_3^-, and 1.7 μM $SO_2^{\bullet-}$) in standard buffer was −530 mV, which was similar to the potential calculated according to the method of Mayhew (*34*). Thus, according to the Nernst equation, 90% of $Av2(MgADP)_2$ will be reduced. This accounts for an ϵ_{430} of 4.10 mM^{-1} cm^{-1}, while a value of 3.53 mM^{-1} cm^{-1} was found experimentally. This value was used in the calculations. A similar observation was made by Ashby and Thorneley (*26*) for the molecular absorbance coefficient for the reduction of $Kp2_{ox}(MgADP)_2$. This value was 80% of the molecular absorbance coefficient for the reduction of $Kp2_{ox}$.

Figure 1B shows that the observed rate constant of the reduction of $Av2_{ox}(MgADP)_2$ increased with the concentration of dithionite ($SO_2^{\bullet-}$). The second-order rate constant for the reduction of $Av2_{ox}(MgADP)_2$ by $SO_2^{\bullet-}$, calculated from the initial linear dependence of k_{obs} on $[SO_2^{\bullet-}]$, is 3×10^6 M^{-1} s^{-1} (valid only at low dithionite concentrations). This value is similar to the value reported for the reduction of $Kp2_{ox}(MgADP)_2$ (*23*, *26*) and is close to the values for k of $(3.2 \pm 0.2) \times 10^6$ M^{-1} s^{-1} and $(4.7 \pm 0.5) \times 10^6$ M^{-1} s^{-1} for the reduction of $Ac2_{ox}(MgADP)_2$ from the vanadium nitrogenase and the molybdenum nitrogenase, respectively, reported by Bergström et al. (*38*). In contrast to the Fe protein from *K. pneumoniae* (*26*), we and Bergström et al. (*38*) observed for *Azotobacter* a deviation from the linearity between the observed rate constant and the concentration of $SO_2^{\bullet-}$. Bergström et al. (*38*) attributed this deviation from linearity to inhibition of the reduction at high ionic strengths. We can exclude this possibility since we kept the ionic strength constant. Thus, $S_2O_4^{2-}$ might inhibit the binding of $SO_2^{\bullet-}$ to $Av2_{ox}(MgADP)_2$ specifically.

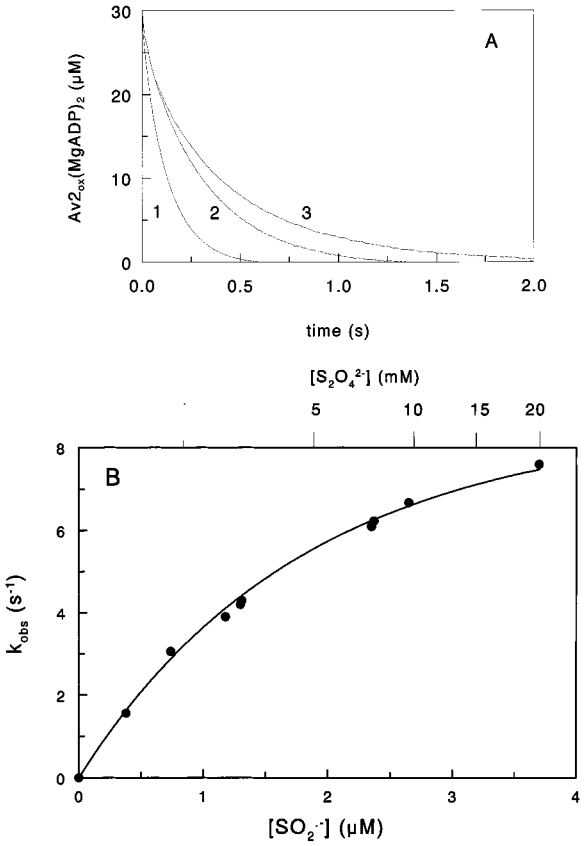

FIGURE 1: Kinetics of the reduction of $Av2_{ox}(MgADP)_2$ by sodium dithionite. (A) Determination of the rate of dissociation of the Av1·$Av2_{ox}(MgADP)_2$ complex in standard buffer. For trace 1, syringe 1 contained 60 μM $Av2_{ox}$ and syringe 2 contained 20 mM $Na_2S_2O_4$. For trace 2, syringe 1 contained 60 μM Av1 and 60 μM $Av2_{ox}$ and syringe 2 contained 432 μM $Av2_{red}$ and 20 mM $Na_2S_2O_4$. For trace 3, syringe 1 contained 60 μM Av1 and 60 μM $Av2_{ox}$ and syringe 2 contained 20 mM $Na_2S_2O_4$. (B) The observed rate constant (k_{obs}) of the reduction of $Av2_{ox}(MgADP)_2$ depends on $[SO_2^{\bullet-}]$. Syringe 1 contained 50 μM $Av2_{ox}$, and syringe 2 contained $Na_2S_2O_4$ (0−40 mM).

Determination of the Rate of Dissociation of the Nitrogenase Complex. The rate of dissociation of $Av2_{ox}(MgADP)_2$ from Av1 was determined as described for the nitrogenase of *K. pneumoniae* (*23*). Av1, $Av2_{ox}$, and MgADP were mixed with 20 mM dithionite, MgADP, and variable concentrations of $Av2_{red}$ (0−432 μM). In this Fe protein cycle model, the Av1·$Av2_{ox}(MgADP)_2$ complex must dissociate (eq 1) before $Av2_{ox}(MgADP)_2$ can be reduced (eq 2). $Av2_{red}(MgADP)_2$ increases the rate of reduction of $Av2_{ox}(MgADP)_2$ by binding to Av1 (eq 3) and thus suppressing the association of Av1 and $Av2_{ox}(MgADP)_2$ (eq 1). At increasing concentrations of $Av2_{red}$, the absorbance decrease curves are increasingly determined by the rate of the

Table 1: Rate Constants Obtained from the Simulation of the Reduction of the Oxidized Fe Protein$(MgADP)_2$−MoFe Protein Complex by Sodium Dithionite at 20 °C

	$Av1{\cdot}Av2_{ox}(MgADP)_2$		$Av1{\cdot}Av2_{red}(MgADP)_2$		$Av1{\cdot}Av2_{ox}(MgADP)_2$		
	rate of dissociation and dissociation constants[a]					quality of fit	
	k (s^{-1})	K_d (μM)	k (s^{-1})	K_d (μM)	rate of reduction k (s^{-1})	R^2	MSE[b]
simulation 1	8.1 ± 0.2	20.8 ± 2.1	98 ± 82	3.3 ± 3.1	−	0.9979	0.331
simulation 2	2.3 ± 0.04	0.8 ± 0.2	95 ± 67	1.2 ± 1.1	1.78 ± 0.01	0.9993	0.117

[a] The rate of dissociation and reduction and the dissociation constants were determined with 10 mM sodium dithionite. [b] MSE is the mean square error (the sum of the squared differences between the experimental and the calculated data points, divided by the amount of variables used in the simulation).

dissociation of the $Av1{\cdot}Av2_{ox}(MgADP)_2$ complex (compare traces 2 and 3 of Figure 1A).

$$Av1{\cdot}Av2_{ox}(MgADP)_2 \leftrightarrow Av1 + Av2_{ox}(MgADP)_2 \quad (1)$$

$$Av2_{ox}(MgADP)_2 + SO_2^{\bullet -} + H_2O \leftrightarrow Av2_{red}(MgADP)_2 + HSO_3^- + H^+ \quad (2)$$

$$Av2_{red}(MgADP)_2 + Av1 \leftrightarrow Av1{\cdot}Av2_{red}(MgADP)_2 \quad (3)$$

The obtained progression curves, as shown in Figure 1A, could be approximated by a single-exponential decay. The estimated pseudo-first-order rate constants of reduction (k_{obs}) of 30 μM $Av2_{ox}(MgADP)_2$ by 10 mM sodium dithionite in the presence of 30 μM Av1 (60 μM Av2 binding sites) varied from 1.8 ± 0.2 s^{-1} in the absence of $Av2_{red}(MgADP)_2$, via k_{obs} = 2.4 ± 0.15 [25 μM $Av2_{red}(MgADP)_2$], k_{obs} = 2.7 ± 0.19 [50 μM $Av2_{red}(MgADP)_2$], and k_{obs} = 3.0 ± 0.17 [80 μM $Av2_{red}(MgADP)_2$], to 3.1 ± 0.2 s^{-1} in the presence of 216 μM $Av2_{red}$. The values are the average of two independent experiments. Our data are comparable with data in the literature, taking into account the fact that our data were obtained at 20 °C while others have measured at 23 °C. Thorneley and Lowe (*23*) reported that the pseudo-first-order rate constant of reduction increased from 1.1 s^{-1} in the absence of $Kp2_{red}(MgADP)_2$ to 3.0 s^{-1} in the presence of 117 μM $Kp2_{red}(MgADP)_2$. Lanzilotta et al. (*19*, *21*) reported values of 6 and 7 s^{-1} for the pseudo-first-order reduction of 20 μM $Av2_{ox}(MgADP)_2$ in the presence of 20 μM Av1, 100 μM $Av2_{red}(MgADP)_2$, and 10 mM sodium dithionite.

The model used to simulate the stopped-flow curves to estimate the rate of dissociation of the nitrogenase complex comprised the reactions in eqs 1−3. In the simulations, a k_{obs} of 6.7 s^{-1} was used for the reduction of $Av2_{ox}(MgADP)_2$ by dithionite; this value was obtained from Figure 1B (10 mM $Na_2S_2O_4$ and 3.3 μM $SO_2^{\bullet -}$). The rate constant of the dissociation of the $Av1{\cdot}Av2_{ox}(MgADP)_2$ complex was taken from the simulation that gave the best fit to the data curves as described above and as shown in Figure 1A. The results of the simulations are summarized in Table 1.

In the first simulation, no reduction of $Av2_{ox}(MgADP)_2$ in the complex was allowed. For the dissociation of the $Av1{\cdot}Av2_{ox}(MgADP)_2$ complex, a k_{dis} of 8.1 ± 0.2 s^{-1} and a K_d of 20.8 ± 2.1 μM were obtained. For the $Av1{\cdot}Av2_{red}(MgADP)_2$ complex, a dissociation rate k_{dis} of 98 ± 82 s^{-1} and a K_d of 3.3 ± 3.1 μM were obtained. The large error in the values of the rate constant of the dissociation and the K_d of the $Av1{\cdot}Av2_{red}(MgADP)_2$ complex indicates that the simulation is not sensitive to the value of the rate constants of eq 3. Surprisingly, although the dissociation of the nitrogenase complex is supposed to be the rate-limiting step of the Fe protein cycle (*23*), the calculated rate constant for the dissociation of the nitrogenase complex from *Azotobacter* (8.1 s^{-1}) was significantly higher than the observed maximum rate of turnover of the Fe protein cycle [3.0 ± 0.4 mol of electrons s^{-1} (mol of Mo)$^{-1}$]. In addition, the simulation predicts a dissociation constant of the $Av1{\cdot}Av2_{ox}(MgADP)_2$ complex (21 μM) which is 10-fold higher than the corresponding dissociation constant reported for the nitrogenase proteins from *K. pneumoniae* (1.5 μM; *23*). These differences are considered too large, and therefore, a second model was examined.

In the second simulation, an extra reaction was added, the reduction of $Av2_{ox}$ in the $Av1{\cdot}Av2_{ox}(MgADP)_2$ complex (Table 1, simulation 2). With this addition, the simulation yielded a k_{dis} of 2.3 ± 0.04 s^{-1} for the rate of dissociation of the $Av1{\cdot}Av2_{ox}(MgADP)_2$ complex and a dissociation constant of 0.8 ± 0.2 μM. The corresponding values for the $Av1{\cdot}Av2_{red}(MgADP)_2$ complex were a k_{dis} of 95 ± 67 s^{-1} and a K_d of 1.2 ± 1.1 μM. The simulation yielded a k_{obs} of 1.78 ± 0.01 s^{-1} for the pseudo-first-order rate of reduction of $Av2_{ox}(MgADP)_2$ in the $Av1{\cdot}Av2_{ox}(MgADP)_2$ complex (Table 1). The addition of the extra variable did increase the quality of the fit, but more importantly, the dissociation constant of the $Av1{\cdot}Av2_{ox}(MgADP)_2$ complex is now in the same range as the constant for the corresponding nitrogenase complex from *K. pneumoniae*.

Reduction of $Av2_{ox}(MgADP)_2$ by Flavodoxin Hydroquinone. The rate of reduction of $Av2_{ox}(MgADP)_2$ by Fld was monitored by the absorbance increase at 580 nm, associated with the oxidation of Fld_{HQ}. The results from a typical experiment are shown in Figure 2A [trace $Av2_{ox}(MgADP)_2$]. The rate of reduction of $Av2_{ox}(MgADP)_2$ by Fld_{HQ} was so fast (k_{obs} = 1018 s^{-1}) that only the last 15% of the total absorbance change could be detected. To be certain about the extent of oxidation, the absorbance at 580 nm of the proteins before mixing or without reaction must be known exactly. This information is very difficult to obtain with reactive proteins such as nitrogenase and Fld_{HQ}. We solved this problem by incubating flavodoxin (∼450 μM) in a redox buffer (5 mM dithionite). When the oxidation of Fld_{HQ} by nitrogenase (∼30 μM $Av2_{ox}$) is fast and the reduction of Fld_{SQ} to Fld_{HQ} by the redox buffer is slow, the oxidation and reduction reactions of flavodoxin can be separated kinetically. This means that after a rapid oxidation by nitrogenase, the redox buffer (5 mM dithionite) will reduce flavodoxin (∼30 μM) back to its original redox state. These required properties are achieved with dithionite. As shown earlier, $S_2O_4^{2-}$ dissociates in $2SO_2^{\bullet -}$. $SO_2^{\bullet -}$ and the oxidant,

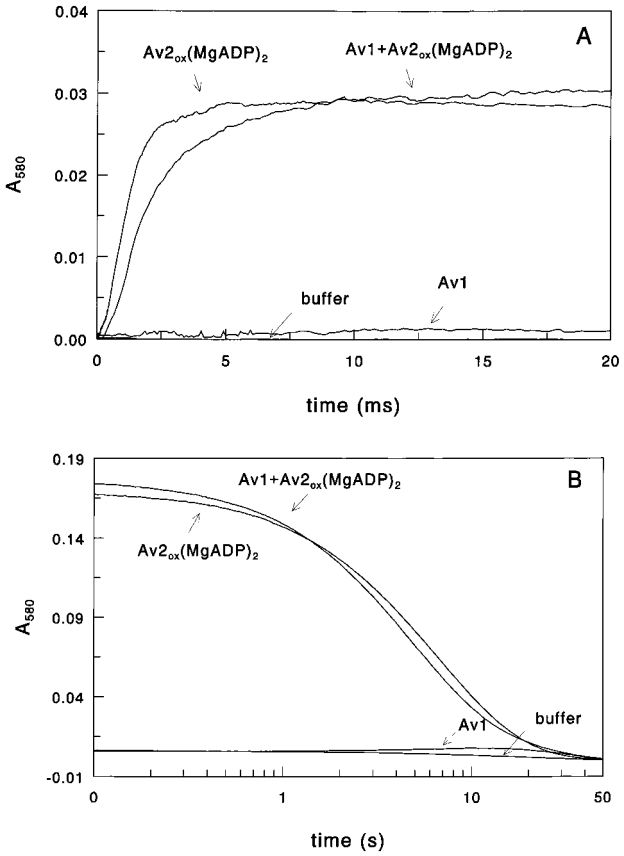

FIGURE 2: Absorbance changes (A_{580}) associated with the oxidation and/or reduction of flavodoxin hydroquinone/semiquinone. (A) The absorbance changes (A_{580}) associated with the oxidation Fld_{HQ} by $Av2_{ox}(MgADP)_2$, in the absence and in the presence of Av1. Syringe 1 contained 60 μM $Av2_{ox}$ for trace $Av2_{ox}(MgADP)_2$, 60 μM Av1 and 60 μM $Av2_{ox}$ for trace $Av1+Av2_{ox}(MgADP)_2$, and 60 μM Av1 for trace Av1. For trace buffer, syringe 1 contained no nitrogenase proteins. Syringe 2 contained 312 μM Fld_{HQ}, 132 μM Fld_{SQ}, and 5 mM $Na_2S_2O_4$. Both syringes contained 1 mM ADP in standard buffer. (B) The absorbance changes (A_{580}) associated with the reduction of Fld_{SQ} by dithionite. Conditions were like those described for panel A.

SO_3^{2-}, are in redox equilibrium with nitrogenase and flavodoxins (*37*−*39*). At 5 mM dithionite, the concentration of the actual reductant, $SO_2^{\bullet-}$, is only 1.9 μM, and with a k of 3.2×10^4 M^{-1} s^{-1}, the reduction of Fld_{SQ} will be slow ($k_{obs} = 0.06$ s^{-1}). This rate can be stimulated about 5 times by free Fe protein (*39*). Thus, by following the absorbance at 580 nm in a stopped-flow experiment of a flavodoxin/dithionite solution at longer reaction times, one can observe the re-reduction of rapidly oxidized Fld_{HQ}. The absorbance traces of the re-reduction of Fld_{SQ} after oxidation by nitrogenase are shown in Figure 2B. From the extent of re-reduction [trace $Av2_{ox}(MgADP)_2$], it is clear that about 30 μM Fld_{HQ} has been oxidized by $Av2_{ox}(MgADP)_2$ within the mixing time of the stopped-flow experiment.

The reduction of $Av2_{ox}(MgADP)_2$ in the presence of Av1 by flavodoxin was also measured [trace $Av1+Av2_{ox}(MgADP)_2$]. Since the rate of reduction of free $Av2_{ox}(MgADP)_2$ by 156 μM Fld_{HQ} ($k_{obs} > 1000$ s^{-1}) is much faster than the expected rate of association of $Av2_{ox}(MgADP)_2$ with Av1, reduction of $Av2_{ox}(MgADP)_2$ bound to Av1 by Fld_{HQ} must be limited by the rate of dissociation of the $Av1{\cdot}Av2_{ox}(MgADP)_2$ complex. This will be the case if reduction in the nitrogenase complex is not possible. As can be seen in Figure 2A, 156 μM Fld_{HQ} reduced 30 μM $Av2_{ox}(MgADP)_2$ in the presence of 30 μM Av1 (60 μM Av2 binding sites) with a k_{obs} of 460 s^{-1} [trace $Av1+Av2_{ox}(MgADP)_2$]. The reaction was so fast that already 80% of the $Av2_{ox}(MgADP)_2$ was reduced within the mixing time of the stopped-flow apparatus. From the re-reduction of Fld_{SQ} by the redox buffer, it can be calculated that 31.6 μM Fld_{HQ} was oxidized in this experiment.

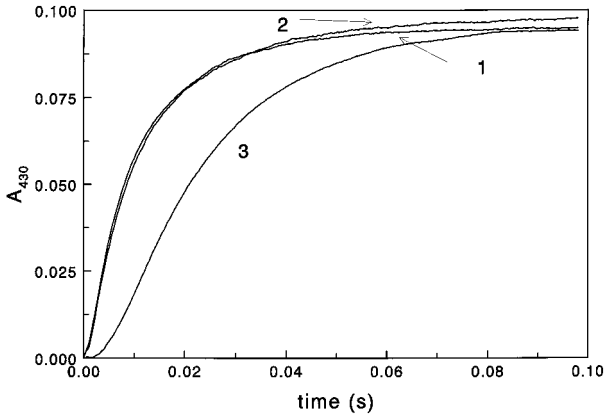

FIGURE 3: Effect of incubation of the nitrogenase proteins with MgADP on the rate of electron transfer between the nitrogenase proteins. The rate of electron transfer was monitored by the absorbance increase at 430 nm. Syringe 1 contained 21 μM Av1 and 135 μM Av2; syringe 2 contained 20 mM ATP and 20 mM $MgCl_2$. Both syringes contained the standard buffer with 5 mM sodium dithionite without ADP: trace 1, no ADP in the reaction mixture; trace 2, 1 mM ADP added to the ATP solution; and trace 3, nitrogenase proteins incubated with 1 mM ADP (before mixing with ATP).

Nucleotide Exchange. The rate of the nucleotide exchange reaction on the reduced nitrogenase complex [$Av1{\cdot}Av2_{red}(MgADP)_2$] was investigated by measuring the effect of an incubation of the reduced nitrogenase proteins with MgADP prior to mixing with MgATP. MgATP brings on electron transfer from the Fe protein to the MoFe protein. Trace 2 of Figure 3 shows that 0.5 mM MgADP did not affect the absorbance changes that accompany the electron transfer. MgADP and MgATP were present in the same syringe. When the nitrogenase proteins were incubated with MgADP before mixing with MgATP however (trace 3), the electron transfer started after a short lag phase (~5 ms) and the observed rate of electron transfer was lowered from 100 to 55 s^{-1}. Thorneley and Cornish-Bowden (*40*) performed a similar type of experiment. When Kp2 saturated with MgADP was mixed with Kp1 and MgATP, a slower rate of electron transfer was found (130 vs 67 s^{-1}) compared with the experiment where MgADP and MgATP were separated from nitrogenase. It is not clear from the presented curves if a lag phase was present. In addition, no simulation of the obtained curve was reported. Our curve with the lag phase (trace 3, $k_{obs} = 55$ s^{-1}) could be simulated with a rate of nucleotide exchange of 70 s^{-1} of the reduced Fe protein bound to the MoFe protein followed by a rate of electron transfer of 100 s^{-1}. The simulated nucleotide exchange rate is still considerably higher than the turnover rate of the Fe protein cycle. Thus, it is clear that the rate of nucleotide exchange of the reduced nitrogenase proteins does not limit the rate of the Fe protein cycle.

Electron Uptake by Nitrogenase during Turnover. More evidence that Fld_{HQ} is capable of reducing the $Av1{\cdot}Av2_{ox}$-

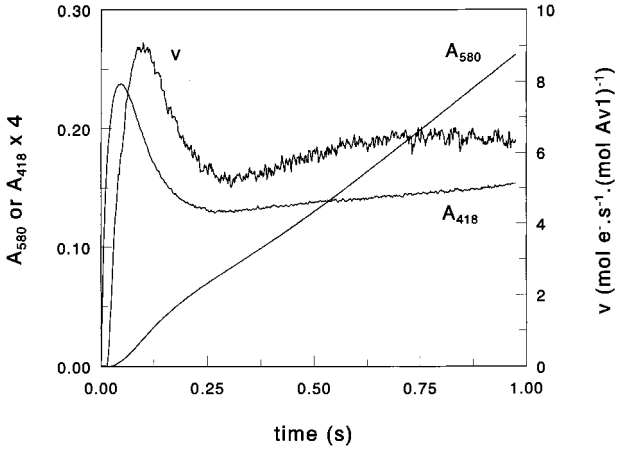

FIGURE 4: Absorbance changes associated with the electron transfer and the oxidation of flavodoxin hydroquinone by nitrogenase during turnover. The rate of electron transfer was monitored by the absorbance increase at 418 nm. The rate of oxidation of Fld_{HQ} was measured by the absorbance increase at 580 nm; v (moles of electrons per ssecond per mole of Mo) is the rate of the oxidation of Fld_{HQ} to Fld_{SQ}. Syringe 1 contained 16 μM Av1 and 96 μM Av2, 370 μM Fld_{HQ}, 150 μM Fld_{SQ}, and 1 mM $Na_2S_2O_4$. Syringe 2 contained 10 mM ATP and 10 mM $MgCl_2$. Both syringes contained the standard buffer without ADP.

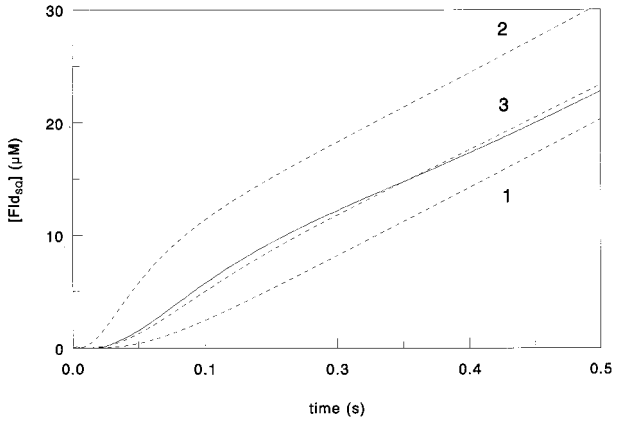

FIGURE 5: Simulation of the pre-steady-state oxidation of Fld_{HQ} to Fld_{SQ} by nitrogenase. The solid trace shows the data of Figure 4. The dotted traces show simulations of the Fe protein cycle with various assumptions: 1, reduction after the rate-limiting step; 2, reduction before the rate-limiting step; and 3, reduction before and after rate-determining steps.

$(MgADP)_2$ complex without a preceding dissociation of the complex was obtained from pre-steady-state kinetic studies of Fld_{HQ} oxidation. The nitrogenase proteins and flavodoxin were in redox equilibrium with sodium dithionite (1−5 mM) in one syringe of the stopped-flow apparatus. In different experiments, the Av1 concentration was varied between 10 and 16 μM, the Av2 concentration was always in a 6-fold excess, and the Fld concentration was varied between 86 and 520 μM. After mixing with MgATP, catalysis starts with reduced proteins. At 418 nm, an isosbestic point of Fld_{HQ}/Fld_{SQ}, the absorbance changes of nitrogenase are observed and the absorbance increase at 580 nm registers the formation of Fld_{SQ} from Fld_{HQ}. Nitrogenase will react mainly with Fld_{HQ} since the concentration of $SO_2^{\bullet-}$ is very low (<1.5 μM). The results from a typical experiment are shown in Figure 4. The electron transfer from Av2 to Av1 is observed immediately after mixing of the nitrogenase proteins with MgATP (increase in the absorbance at 418 nm). This reaction is complete within 50 ms. After a lag of about 20 ms, the oxidation of Fld_{HQ} started (observed as an increase of the absorbance at 580 nm), leading to a fast oxidation phase. The rate of formation of Fld_{SQ} was calculated from the tangent to the absorbance changes at 580 nm. In this phase, the absorbance at 418 nm decreases which indicates reduction and a blue shift of the Fe−S cluster absorbance of nitrogenase (*29*). A slower phase and the steady state follow the phase with the maximal rate of uptake of electrons from FldHQ. After 300 ms, 1 mol of Fld_{HQ} per mole of Mo was oxidized. The maximal rate of electron uptake was 4.9 mol of electrons s^{-1} (mol of Mo)$^{-1}$ in the pre-steady state and 3.6 mol of electrons s^{-1} (mol of Mo)$^{-1}$ in the steady state. In this experiment, the protein ratio of [Av2]/[Av1] equals 6, which explains the slightly lower steady-state rate as compared to the value of 4.0 mol of electrons s^{-1} (mol of Mo)$^{-1}$, obtained with a [Av2]/[Av1] ratio of 20 at low MoFe protein concentrations. To gain insight into the timing of the reduction taking place within the nitrogenase complex after electron transfer, the formation of Fld_{SQ} in the pre-steady state was simulated with different kinetic models for the Fe protein cycle (see Figure 5). The basic model consists of complex formation, electron transfer, on-enzyme MgATP hydrolysis (delay reaction), and H^+ (P_i) release. How the Fe protein cycle proceeds after these reactions is not clear. For the sake of simplicity, we used in the simulation one slow reaction (5 s^{-1}) to obtain the experimentally determined rate of the cycle. This reaction can be a conformational change in the nitrogenase complex, or dissociation of the nitrogenase complex. If we assume that the reduction takes place after the slow step (5 s^{-1}), the simulations do not follow the experimental data (Figure 5, trace 1). If we assume that reduction takes place after P_i and/or H^+ release and before the slow step, the simulation produced curve 2. To obtain a reasonable simulation of the data curve, two slow steps must be included in the model (curve 3). One step (15.7 s^{-1}) occurs immediately after the P_i and/or H^+ release reaction, and then the reduction reaction which is followed by a reversible reaction with a $k_{forward}$ of 10.5 s^{-1} and a $k_{backward}$ of 16.1 M^{-1} s^{-1}. This reversible reaction might be the dissociation of the reduced nitrogenase complex.

DISCUSSION

It is proposed in the literature that the rate-limiting step of the Fe protein cycle (Scheme 1), and thus of nitrogenase catalysis, is the dissociation of the nitrogenase complex. Dissociation is thought to be obligatory for the reduction of the Fe protein and for the subsequent exchange of MgATP for MgADP (*22*, *23*, *26*). We determined the rate of dissociation of the $Av1{\cdot}Av2_{ox}(MgADP)_2$ complex according to the method described in the literature (*23*). The data were analyzed with two models. The model with no reduction in the complex requires a dissociation constant of the $Av1{\cdot}Av2_{ox}(MgADP)_2$ complex with a magnitude higher than that of the dissociation constant of the corresponding nitrogenase complex from *K. pneumoniae* (K_d = 20.8 and 1.5 μM, respectively) (*23*). An alternative model (Table 1, simulation 2) includes reduction of $Av2_{ox}$ in the $Av1{\cdot}Av2_{ox}(MgADP)_2$ complex, besides the reduction of $Av2_{ox}(MgADP)_2$ after the dissociation of the complex. If this is allowed, the dissociation constant of the $Av1{\cdot}Av2_{ox}(MgADP)_2$ complex has values with the same magnitude as the corresponding value

Scheme 2: Extended Fe Protein Cycle of *A. vinelandii* Nitrogenase[a]

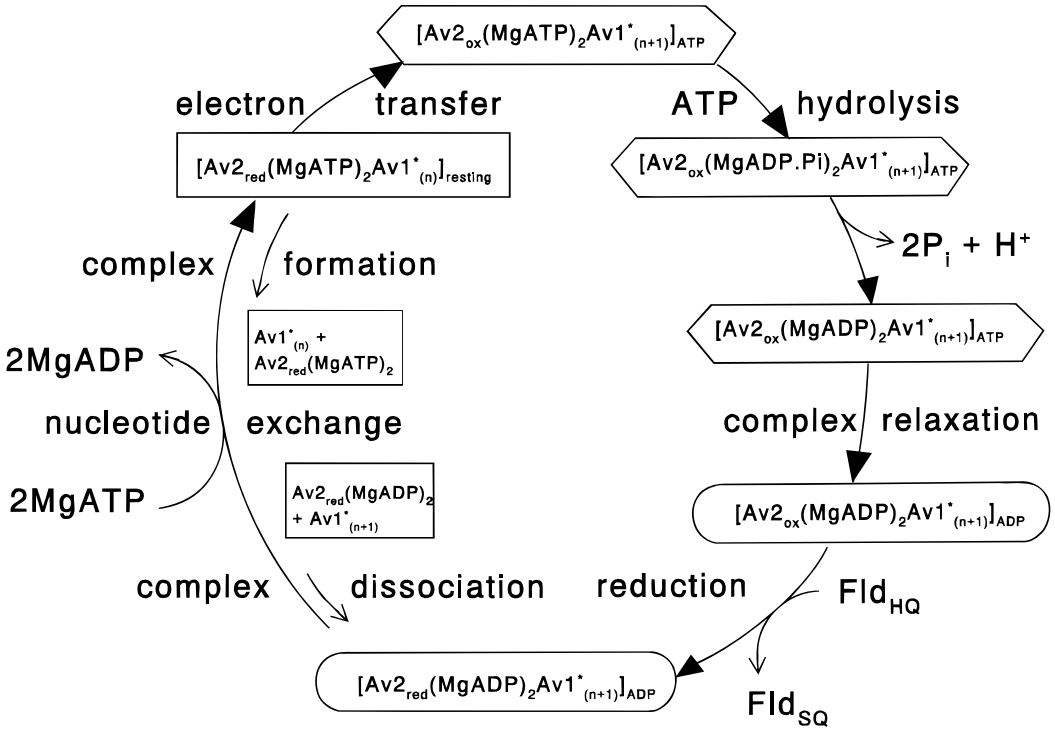

[a] Av1* is one of the two independently functioning halves of Av1. $Av1^*_n$ is Av1* reduced by *n* electrons. $[Av2(MgATP)_2Av1^*]_{resting}$, $[Av2(MgATP)_2Av1^*]_{ATP}$, or $[Av2(MgADP)_2Av1^*]_{ADP}$ is the nitrogenase complex in a resting-state, MgATP-bound, or MgADP-bound conformation, respectively. For details and rate constants, see the text.

from *K. pneumoniae* (K_d = 0.8 and 1.5 μM, respectively). We also fitted the two used models to the data published by Thorneley and Lowe (*23*). From the computer best fits, we obtained about the same values that have been published and observed that FITSIM made the rate constant for reduction of $Kp2_{ox}$ in the complex zero. This means that the reduction of $Kp2_{ox}$ in the complex is not necessary to fit the data of *Klebsiella* nitrogenase. Reduction of the *Azotobacter* Fe protein in the nitrogenase complex has been suggested earlier.

Hageman and Burris (*41*) compared several models of possible functional nitrogenase complexes with the obtained steady-state kinetics. Their major conclusions were that the catalytic complex is a transient one and that dithionite is a relatively poor reductant for *Azotobacter* nitrogenase whereas flavodoxin is much better. Since they used steady-state kinetics, it was not possible to determine individual rate constants of the different proposed reactions such as reduction of the free Fe protein and the Fe protein bound to the MoFe protein and dissociation of the nitrogenase complex. Druzhinin et al. (*42*) demonstrated directly that the photochemical electron donor eosin-NADH reduced Av2 in the complex as efficiently as free Av2. Lanzilotta and Seefeldt (*20*) showed that flavodoxin can reduce the [4Fe-4S] cluster of the L127Δ Fe protein bound to the MoFe protein whereas dithionite cannot. By comparing dithionite with flavodoxin, one has to realize that at 5 mM dithionite the actual concentration of the reductant, $SO_2^{\bullet-}$, is only 2.4 μM, while flavodoxin is normally used at concentrations of about 100 μM. It is possible that this concentration effect seems to make flavodoxin a more powerful reductant compared with dithionite.

The simulations of the dithionite reduction data might suggest that dithionite can reduce the Fe protein in the nitrogenase complex, but the data presented in Figures 2 and 4 clearly show that Fld_{HQ} indeed can reduce the nitrogenase complex. One can argue that Fld_{HQ} stimulates dissociation of the nitrogenase complex, after which Fld_{HQ} rapidly reduces the free Fe protein. We think that this explanation is unlikely. If this explanation would be true, flavodoxin would stimulate the Fe protein cycle significantly compared with dithionite. The reason is that after the very fast flavodoxin-induced dissociation and reduction, the nucleotide exchange on the reduced Fe protein (70 s^{-1}) is the last reaction before the next round of the Fe protein cycle. According to the models of the Fe protein cycle, this would bypass the rate-limiting step and thus stimulate the rate of the Fe protein cycle, which is not observed. Using flavodoxin instead of sodium dithionite stimulates the rate of the Fe protein cycle only from 3 to 4 s^{-1}.

We think that our data show that dissociation of the nitrogenase complex is not necessary for reduction by flavodoxin, but on the other hand, we cannot exclude the possibility that dissociation of the reduced nitrogenase proteins is still an essential reaction of the Fe protein cycle. The data curve of Figure 3 (trace 3) could be fitted with a nucleotide exchange rate of 70 s^{-1} followed by an electron transfer reaction of 100 s^{-1}. It is possible that the rate of this exchange reaction is determined by the rate of dissociation of the reduced complex followed by a rapid nucleotide exchange. Another explanation might be that it represents a nucleotide exchange on the reduced complex. As discussed before, the simulation of the dissociation reactions is not sensitive to the rate of dissociation of the reduced complex. Therefore, it is not possible with our data to exclude a rate of dissociation of the reduced nitrogenase complex of 70 s^{-1}. But also, nucleotide exchange on the nitrogenase

complex cannot be excluded. Lanzilotta et al. (*21*) have shown that nucleotide exchange is possible on a stable nitrogenase complex. They showed that the nondissociable D39N Fe protein−MoFe protein complex has a significant steady-state ATPase activity. If the nucleotide exchange reaction occurs on the reduced nitrogenase complex, the proposed obligatory association and dissociation of the nitrogenase proteins during catalysis are not necessary with flavodoxin as the reductant. The absence of an obligatory dissociation reaction nicely explains why nitrogenase in intact *Azotobacter* cells and *Rhizobium* bacteroids is not inhibited despite the fact that the concentration of nitrogenase is in the range of 40−400 μM (*43*, *44*).

We include the flavodoxin kinetics in an updated version of the Fe protein cycle scheme (Scheme 2). It is known from other ATPases that the hydrolysis of MgATP consists of four distinct steps: the binding of MgATP to the protein, the on-enzyme hydrolysis of MgATP, the release of P_i and H^+, and the release of MgADP. As proposed previously by us (*28*), the binding of MgATP to the reduced nitrogenase complex induces a conformational change of the nitrogenase complex that causes electron transfer from the Fe protein to the MoFe protein. Others suggest that binding of MgATP to the Fe protein is necessary for priming the Fe protein for the proper docking to the MoFe protein which is followed by electron transfer (*1*, *3*, *45*). We doubt if there is kinetic evidence for this "priming" hypothesis. Stopped-flow experiments by Thorneley (*46*) show that the order of mixing does not affect the pre-steady-state electron transfer reaction. Thorneley concluded from his studies that it is not possible to determine the order of assembly of the Fe protein−MoFe protein−MgATP complex and in particular whether complex formation between the Fe and MoFe protein is induced by MgATP. As far as we know, there are no new (kinetic) data that prove or disprove one of the possibilities mentioned above. In addition, the effect of the protein concentration on the rate of electron transfer can be used to estimate the rate of association and dissociation of the nitrogenase complex in the presence MgATP (*25*). Since no lag phase was observed in the electron transfer reaction, it must be concluded that MgATP binds to a preformed complex. If no complex was present before mixing, unrealistically high values ($k_{ass} \geq 10^8$ M^{-1} s^{-1}) for the rate of association of the two nitrogenase proteins must be assumed to fit the data. We were able to confirm these data for *Azotobacter* nitrogenase (*4*). The pre-steady-state electron transfer reaction at low protein concentrations (2.5 μM Av1 and 2.5 μM Av2 were mixed with 10 mM MgATP) is only carried out with a preformed protein complex with a K_D of <0.3 μM. This means that under the conditions of a typical stopped-flow experiment (15 μM Av1 and 90 μM Av2), the Fe protein binding sites on the MoFe protein are almost completely saturated (99% saturation). Therefore, it is likely that MgATP binds rapidly to an Fe protein−MoFe protein complex. The conformation of this complex is called the resting conformation. After binding of MgATP to the Fe protein in the Fe protein−MoFe protein complex, the essential conformational changes occur that are obligatory for electron transfer. The release of P_i (*30*) and H^+ (*28*) and a blue shift of the absorbance maximum, from 430 to 360 nm (*29*), are observed after a lag phase of 15−20 ms. A kinetic analysis of the last three reactions of nitrogenase is consistent with a model which comprises a rapid binding of MgATP to the nitrogenase complex, a change of the conformation of the nitrogenase−MgATP complex allowing electron transfer (100 s^{-1}), and a delay reaction (on-enzyme hydrolysis of MgATP, $k = 77$ s^{-1}) followed by a change of the conformation of the nitrogenase complex (monitored by H^+ release and a blue shift of the absorbance at 430 nm, $k_{obs} = 14$ s^{-1}). A similar kinetic scheme was used by Lowe et al. (*29*) to explain the pre-steady-state P_i release by *K. pneumoniae* nitrogenase. As shown in this paper, Fld_{HQ} rapidly reduces the $Av1{\cdot}Av2_{ox}(MgADP)_2$ complex. The time course of the Fld_{HQ} oxidation during turnover (see Figures 4 and 5) is consistent with a model where reduction of the $Av1{\cdot}Av2_{ox}(MgADP)_2$ complex takes place after the H^+ release reaction (14 s^{-1}) and a hypothetical reaction (15.7 s^{-1}), here depicted as a complex relaxation reaction from the ATP- to the ADP-bound conformation, and before a reversible slow step which could be the dissociation of the reduced nitrogenase complex ($k_{dis} = 10.5$ s^{-1}, $k_{ass} = 16.1$ M^{-1} s^{-1}). Due to the large standard deviation in the calculated rate of the simulations of the dithionite reduction data, we cannot exclude these values for the calculation of the rate of dissociation and association of the reduced proteins with MgADP bound. Further research, for instance, kinetic studies with altered proteins that are blocked in a specific conformation which is necessary to proceed through the Fe protein cycle, will help to unravel the reactions that close the Fe protein cycle.

ACKNOWLEDGMENT

We thank Prof. Colja Laane for critically reading the manuscript.

REFERENCES

1. Howard, J. B., and Rees, D. C. (1994) *Annu. Rev. Biochem. 63*, 235−264.
2. Peters, J. W., Fisher, K., Newton, W. E., and Dean, D. R. (1995) *J. Biol. Chem. 270*, 27007−27013.
3. Lanzilotta, W. N., and Seefeldt, L. C. (1996) *Biochemistry 35*, 16770−16776.
4. Duyvis, M. G., Mensink, R. E., Wassink, H., and Haaker, H. (1997) *Biochim. Biophys. Acta 1320*, 34−44.
5. Kim, J., and Rees, D. C. (1992) *Science 257*, 1677−1682.
6. Bolin, J. T., Campobasso, N., Muchmore, S. W., Morgan, T. V., and Mortenson, L. E. (1993) in *Molybdenum enzymes, cofactors and model systems* (Stiefel, E. I., Coucouvanis, D., and Newton, W. E., Eds.) pp 186−195, American Chemical Society, Washington, DC.
7. Peters, J. W., Stowell, M. H. B., Soltis, S. M., Finnegan, M. G., Johnson, M. K., and Rees, D. C. (1997) *Biochemistry 36*, 1180−1187.
8. Georgiadis, M. M., Komiya, H., Chakrabarti, P., Woo, D., Kornuc, J. J., and Rees, D. C. (1992) *Science 257*, 1653−1659.
9. Wolle, D., Dean, D. R., and Howard, J. B. (1992) *Science 258*, 992−995.
10. Rayment, I., Holden, H. M., Whittaker, M., Yohn, C. B., Lorenz, M., Holmes, K. C., and Milligan, R. A. (1993) *Science 261*, 58−65.
11. Sondek, J., Lambright, D. G., Noel, J. P., Hamm, H. E., and Sigler, P. B. (1994) *Nature 372*, 276−279.
12. Coleman, D. E., Berghuis, A. M., Lee, E., Linder, M. E., Gilman, A. G., and Sprang, S. R. (1994) *Science 265*, 1405−1412.
13. Duyvis, M. G., Wassink, H., and Haaker, H. (1996) *FEBS Lett. 380*, 233−236.

14. Renner, K. A., and Howard, J. B. (1996) *Biochemistry 35*, 5353−5358.
15. Mittal, R., Ahmadian, M. R., Goody, R. S., and Wittinghofer, A. (1996) *Science 273*, 115−117.
16. Schindelin, H., Kisker, C., Schlessman, J. L., Howard, J. B., and Rees, D. C. (1997) *Nature 387*, 370−376.
17. Scheffzek, K., Ahmadian, M. R., Kabsch, W., Wiesmüller, L., Lautwein, A., Schmitz, F., and Wittinghofer, A. (1997) *Science 277*, 333−338.
18. Ryle, M. J., and Seefeldt, L. C. (1996) *Biochemistry 35*, 4766−4775.
19. Lanzilotta, W. N., Fisher, K., and Seefeldt, L. C. (1996) *Biochemistry 35*, 7188−7196.
20. Lanzilotta, W. N., and Seefeldt, L. C. (1997) *Biochemistry 36*, 12976−12983.
21. Lanzilotta, W. N., Fisher, K., and Seefeldt, L. C. (1997) *J. Biol. Chem. 272*, 4157−4165.
22. Hageman, R. V., and Burris, R. H. (1978) *Proc. Natl. Acad. Sci. U.S.A. 75*, 2699−2702.
23. Thorneley, R. N. F., and Lowe, D. J. (1983) *Biochem. J. 215*, 393−403.
24. Lowe, D. J., and Thorneley, R. N. F. (1984) *Biochem. J. 224*, 877−886.
25. Lowe, D. J., and Thorneley, R. N. F. (1984) *Biochem. J. 224*, 895−901.
26. Ashby, G. A., and Thorneley, R. N. F. (1987) *Biochem. J. 246*, 455−465.
27. Thorneley, R. N. F., and Lowe, D. J. (1984) *Biochem. J. 224*, 887−894.
28. Duyvis, M. G., Wassink, H., and Haaker, H. (1994) *Eur. J. Biochem. 225*, 881−890.
29. Duyvis, M. G., Wassink, H., and Haaker, H. (1996) *J. Biol. Chem. 271*, 29632−29636.
30. Lowe, D. J., Ashby, G. A., Brune, M., Knights, H., Webb, M. R., and Thorneley, R. N. F. (1995) in *Nitrogen fixation: fundamentals and applications* (Tikhonovich, I. A., Provorov, N. A., Romanov, V. I., and Newton, W. E., Eds.) pp 103−108, Kluwer Academic Publishers, Dordrecht, The Netherlands.
31. Mensink, R. E., Wassink, H., and Haaker, H. (1992) *Eur. J. Biochem. 208*, 289−294.
32. Braaksma, A., Haaker, H., Grande, H. J., and Veeger, C. (1982) *Eur. J. Biochem. 121*, 483−491.
33. Klugkist, J., Voorberg, J., Haaker, H., and Veeger, C. (1986) *Eur. J. Biochem. 155*, 33−40.
34. Mayhew, S. G. (1978) *Eur. J. Biochem. 85*, 535−547.
35. Barshop, B. A., Wrenn, R. F., and Frieden, C. (1983) *Anal. Biochem. 130*, 134−145.
36. Zimmerle, C. T., and Frieden, C. (1989) *Biochem. J. 258*, 381−387.
37. Deistung, J., and Thorneley, R. N. F. (1986) *Biochem. J. 239*, 69−75.
38. Bergström, J., Eady, R. R., and Thorneley, R. N. F. (1988) *Biochem. J. 251*, 165−169.
39. Thorneley, R. N. F., and Deistung, J. (1988) *Biochem. J. 253*, 587−595.
40. Thorneley, R. N. F., and Cornish-Bowden, A. (1977) *Biochem. J. 165*, 255−262.
41. Hageman, R. V., and Burris, R. H. (1978) *Biochemistry 17*, 4117−4124.
42. Druzhinin, S. Yu., Syrtsova, L. A., Rubtsova, E. T., and Shkondina, N. I. (1996) *Biochemistry (Moscow) 61*, 1567−1574.
43. Klugkist, J., Haaker, H., Wassink, H., and Veeger, C. (1985) *Eur. J. Biochem. 146*, 509−515.
44. Haaker, H., and Wassink, H. (1984) *Eur. J. Biochem. 142*, 37−42.
45. Seefeldt, L. C., Ryle, M. J., Chan, J. M., and Lanzilotta, W. N. (1998) in *Biological Nitrogen Fixation for the 21st Century* (Elmerich, C., Kondorosi, A., and Newton, W. E., Eds.) pp 39−42, Kluwer Academic Publishers, Dordrecht, The Netherlands.
46. Thorneley, R. N. F. (1975) *Biochem. J. 145*, 391−396.

BI981509Y